Materials Science in Semiconductor Processing 39 (2015) 755–759

Contents lists available at ScienceDirect

Materials Science in Semiconductor Processing

journal homepage: www.elsevier.com/locate/matsci

Influence of the indium nominal concentration in the formation of $CuInS_2$ films grown by CBD

F. de Moure-Flores [a,*], A. Guillén-Cervantes [b], E. Campos-González [b], J. Santoyo-Salazar [b], J.S. Arias-Cerón [c], J. Santos-Cruz [a], S.A. Mayén-Hernández [a], M. de la L. Olvera [c], J.G. Mendoza-Álvarez [b], O. Zelaya-Angel [b], G. Contreras-Puente [d]

[a] Facultad de Química, Materiales, Universidad Autónoma de Querétaro, Querétaro 76010, México
[b] Departamento de Física, CINVESTAV-IPN, Apdo. Postal 14-740, México D.F. 07360, México
[c] Departamento de Ingeniería Eléctrica, Sección de Estado Sólido, CINVESTAV-IPN, Apdo. Postal 14-740, México D.F. 07360, México
[d] Escuela Superior de Física y Matemáticas del IPN, México D.F. 07738, México

ARTICLE INFO

Article history:
Received 18 February 2015
Received in revised form
29 May 2015
Accepted 13 June 2015

Keywords:
$CuInS_2$ films
PL at room temperature
$CuInS_2$ nanotubes
Chemical bath deposition

ABSTRACT

Copper indium disulfide ($CuInS_2$) thin films were prepared by chemical bath deposition in an acid medium on glass substrates. $CuInS_2$ films were grown using $CuSO_4$, $InCl_3$ and C_2H_5NS as copper, indium and sulfur sources, respectively. The $CuSO_4$ and C_2H_5NS concentrations remained constant, while the $InCl_3$ concentration was varied from 0.002 M to 0.025 M. The structural analysis show that initially the films have a mixture of CuS and $CuInS_2$ phases, when the indium nominal concentration increases the formation of $CuInS_2$ ternary compound was promoted until the final formation of a $CuInS_2$ film. The morphological study shows that the surface of $CuInS_2$ films is constituted by nanotubes. The structural and compositional analysis show that for 0.025 M $InCl_3$ concentration $CuInS_2$ films were obtained.

1. Introduction

Copper indium disulfide ($CuInS_2$) films are one of the promising absorber materials in solar cells because of its high absorption coefficient and a direct bandgap of 1.4–1.5 eV [1], also, this material has the advantage that it does not contain toxic elements. Thereby, this material is ideal for production of photovoltaic devises. The stable structure at room temperature of $CuInS_2$ is the chalcopyrite structure with eight atoms per unit cell. A variety of techniques have been used for the $CuInS_2$ thin films deposition; sputtering [2], co-evaporation [3], spray pyrolysis [4] and chemical bath deposition [5] among others. Chemical bath deposition (CBD) is an attractive method because films of large-area can be obtained at low cost. CBD technique involves mixing aqueous solutions of precursor salts of the material to deposit. For the growth of $CuInS_2$ thin films by this technique, aqueous solutions of $InCl_3$, $CuSO_4$ and C_2H_5NS as indium (In), copper (Cu) and sulfur (S) sources, respectively, may be used. In the growth of $CuInS_2$ films by CBD, triethanolamine normally is used as complexing agent to copper and indium [6]. On other hand, one of the problems that ternary compounds present is the control of the stoichiometry. In order to control the stoichiometry of the $CuInS_2$ films obtained by CBD, in this paper we propose to vary the concentration of the In source while the Cu and S source concentrations remain constant. In this work, we report on the influence of the indium nominal concentration in the bath on physical properties of copper indium disulfide (CIS) films grown by CBD. It is important to mention that complexing agents for Cu and In were not used in the processing of our $CuInS_2$ films.

2. Experimental details

2.1. Growth of $CuInS_2$ films

$CuInS_2$ thin films were grown on 2.54 cm × 2.54 cm glass substrates by CBD at a temperature of 70 °C. Before growth, substrates were cleaned in ultrasonic bath for 5 min by rinsing in successive steps in xylenes, ethanol and acetone. The reaction solution was prepared mixing appropriate amounts of $InCl_3$, $CuSO_4$, CH_3COOH and C_2H_5NS. $InCl_3$, $CuSO_4$ and C_2H_5NS were employed as indium, copper and sulfur sources, respectively. $CuSO_4$ and C_2H_5NS concentrations were kept constant at 0.025 M and 0.75 M, respectively. The indium nominal concentration was varied by changing

* Corresponding author.
E-mail address: fcomoure@hotmail.com (F. de Moure-Flores).

http://dx.doi.org/10.1016/j.mssp.2015.06.053
1369-8001/

Table 1
Lattice parameter of hexagonal CuS and tetragonal $CuInS_2$ structures.

Sample	$[InCl_3]$ (M)		Hexagonal CuS			Tetragonal $CuInS_2$		
			a (Å)	c (Å)	V (Å^3)	a (Å)	c (Å)	V (Å^3)
PDF[a]	–	–	3.7920	16.3440	203.52	5.5230	11.1410	339.84
CIS-1	0.002	100	3.7921	16.6889	207.83	5.3608	12.0245	345.56
CIS-2	0.010	158	3.7921	15.9280	190.35	5.3629	12.0126	345.49
CIS-3	0.020	190	3.8237	13.6352	172.64	5.4076	11.7720	344.24
CIS-4	0.025	200	3.8589	12.5468	161.80	5.4595	11.5166	343.26

[a] PDF#06-0464 for hexagonal CuS and PDF#27-0159 for tetragonal $CuInS_2$.

the $InCl_3$ concentration in the bath, $InCl_3$ concentrations used were: 0.002 M, 0.010 M, 0.020 M and 0.025 M. Deionized water (18 MΩ) was used for the preparation of solutions. Reagents were from Sigma-Aldrich with a purity $>$ 99.0%. Complexing agents for the copper and indium were not added to the bath, as mentioned before. The growth time was 1 h and the pH of bath 2. Films were labeled from low to high $InCl_3$ concentration as: CIS-1, CIS-2, CIS-3 and CIS-4 (see Table 1).

The decomposition of thioacetamide in the aqueous medium is as follows [6]:

$$CH_3CSNH_2 \leftrightarrow CH_3C(SH)NH \quad (1)$$

The protonation from acetic acid forms: $CH_3C(SH)NH + H^+ \leftrightarrow CH_3C(H_2S^+)NH$, which dissociates to give H_2S as

$$CH_3C(H_2S^+)NH \rightarrow CH_3CNH^+ + H_2S \quad (2)$$

In an aqueous medium, the H_2S dissociates as

$$H_2S + H_2O \rightarrow HS^- + H_3O^+ \quad (3)$$

$$HS^- + H_2O \rightarrow S^{2-} + H_3O^+ \quad (4)$$

Then, ion-by-ion deposition mechanism occurs between copper, indium and sulfur ions

$$Cu^{2+} + In^{2+} + 2S^{2-} \rightarrow CuInS_2 \quad (5)$$

2.2. Film characterization

Raman spectroscopy measurements were carried out in a Labram Dilor micro-Raman system, employing a HeNe laser (632.8 nm) as excitation source. X-ray diffraction (XRD) patterns were obtained in a Rigaku Smartlab diffractometer, using the Cu-Kα line (1.5406 Å). The films thickness were measured with a KLA Tencor P15 perfilometer. Atomic concentration measurements of films were determined by Energy Dispersive Spectrometry (EDS) with a Bruker 5010 XFlash detector installed in a JEOL JSM-6300 scanning electron microscope (SEM). Photoluminescence (PL) spectra were obtained at room temperature using an Omnichrome-Series 56 He–Cd laser with the 325 nm line.

3. Results and discussion

3.1. Raman study

Fig. 1 shows the Raman spectra of the CIS samples. It can be observed that the indium nominal concentration has strong influence on Raman spectra. The Raman spectrum of the CIS-1 sample has three shoulders at 291 cm^{-1}, 337 cm^{-1} and 469 cm^{-1}. CIS-2 sample has three shoulders at 292 cm^{-1}, 334 cm^{-1} and 470 cm^{-1}. The Raman spectrum 1(c) (sample CIS-3) presents

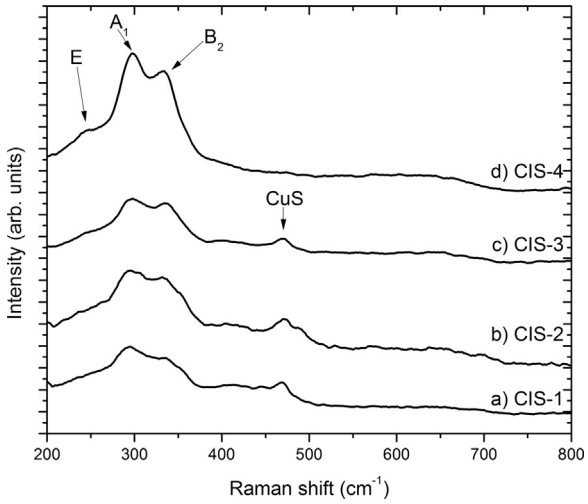

Fig. 1. Raman spectra of CIS films grown by CBD. Note the change in the Raman signal as the In nominal concentration increased in bath.

signals at 297 cm^{-1}, 337 cm^{-1} and 470 cm^{-1}. Finally, in the CIS-4 sample the shoulders are observed at 242 cm^{-1}, 298 cm^{-1} and 337 cm^{-1}. The signals at 291–292 cm^{-1} and 337 cm^{-1} correspond to A_1 and B_2 modes of the $CuInS_2$ [7,8], respectively, while the shoulder at $\approx$470 cm^{-1} corresponds to the CuS [9] phase. The shoulder at $\approx$300 has been reported in Cu poor $CuInS_2$ films, i.e. with indium excess [10]. The shoulder at 242 cm^{-1} of the CIS-4 sample corresponds to E mode of $CuInS_2$ [7]. From Raman spectra observe that when the indium nominal concentration increased the intensity of Raman peak at $\approx$470 cm^{-1} (corresponding to the CuS phase) disappears, which indicates that increasing the In nominal concentration promotes the formation of the $CuInS_2$ (ternary) compound. It is important to note that the Raman spectrum of the CIS-4 sample only present Raman modes assigned to $CuInS_2$ compound and these signals are well defined. These results also indicate that the CIS-4 sample, grown with a 0.025 M $InCl_3$ concentration, corresponds to a $CuInS_2$ film.

3.2. X-ray diffraction characterization

To verify the formation of the $CuInS_2$ compound, XRD measurements were carried out to CIS films. XRD patterns of samples are shown in Fig. 2. The diffractogram 2(a) has four diffraction peaks at 27.80°, 29.20°, 31.68° and 47.94°. The diffraction peaks at 29.20°, 31.68° and 47.94° correspond to CuS covellite phase and diffraction planes are: (102), (103) and (110), while the peak at 27.80° corresponds to the (112) plane of the $CuInS_2$ phase. Therefore, the CIS-1 sample has a mixture of CuS and $CuInS_2$ phases. The diffractogram 2(b) exhibits three peaks at 27.80°, 29.20° and 47.94° (discussed above), indicating that the CIS-2 sample also has a mixture of phases. The diffraction pattern of CIS-3 sample (Fig. 2c) has two peaks at 27.80° and 47.52°. The peak at

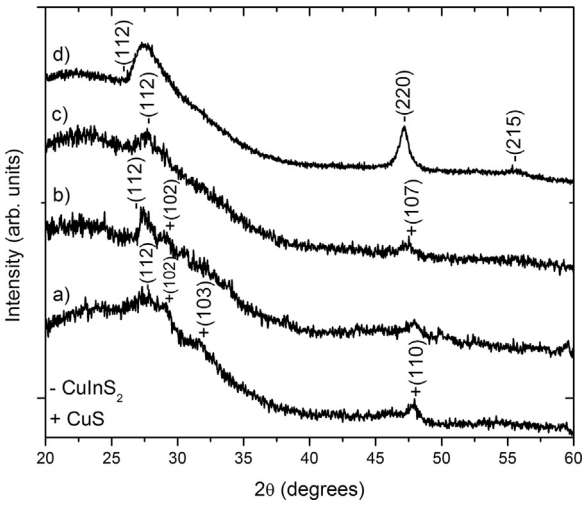

Fig. 2. XRD patterns of CIS films. The diffractogram 2(d) confirms the formation of the $CuInS_2$ compound.

27.80° is assigned to (112) diffraction plane of the tetragonal $CuInS_2$ phase, whereas the peak at 47.52° corresponds to CuS covellite and the diffraction peak is the (107). Finally, the diffraction pattern 2(d) (CIS-4 sample) has three diffraction peaks centered at 27.70°, 47.04° and 55.40° (of very low intensity) and diffraction planes are (112), (220) and (215) of the tetragonal $CuInS_2$, indicates that for a 0.025 M $InCl_3$ concentration $CuInS_2$ films were obtained (in agreement with the Raman study). The peaks were indexed using the powder diffraction files PDF#27-0159 ($CuInS_2$) and PDF#06-0464 (hexagonal CuS). From XRD patterns lattice parameters were calculated, see Table 1. These parameters were calculated to both hexagonal CuS and tetragonal $CuInS_2$ crystalline structures. In the case of the hexagonal CuS structure, the CIS-1 sample has a lattice volume of 207.83 $Å^3$ and the lattice volume decreases as the $InCl_3$ concentration increases. It is important to note that the lattice volume of the CIS-1 sample is very similar to the hexagonal CuS reference (PDF#06-0564). For the case of tetragonal $CuInS_2$ structure, the lattice volume decreases from 345.56 $Å^3$ (CIS-1 sample) to 343.26 $Å^3$ (CIS-4 sample). The lattice volume of the CIS-4 sample is the more similar to tetragonal $CuInS_2$ reference (PDF#27-0159). The crystallite size was calculated using the Scherrer formula: $D=0.9\lambda/B\cos\theta_B$, where D is the crystallite size, λ is the wavelength (1.5406 Å), B is the full width al half maximum (FWHM) of the diffraction peak and θ_B is the Bragg angle. The crystalline size decreases from 22.49 nm to 13.39 nm (see Table 2). The dislocation density and the micro-strain were estimated using the formulas $\delta=n/D^2$ and $\varepsilon=B\cot\theta_B/4$, respectively. Where: δ is the dislocation density, n a factor that when has a value of 1 gives the minimum of dislocation density and ε is the micro-strain. The dislocation density and micro-strain are displayed in Table 2. The δ and ε increase as the $InCl_3$ concentration in the bath increases. We explain this behavior as follows: initially a thin film with a mixture of CuS and $CuInS_2$ phases is formed, however this film (CIS-1 sample) has a great contribution of the CuS phase. As the $InCl_3$ concentration increases, more indium is incorporated in the CuS lattice until the indium amount in the bath is sufficient to form the $CuInS_2$ compound. The indium incorporation in the CuS lattice produces that the dislocation density and micro-strain increases until the $CuInS_2$ compound is formed.

Film thicknesses are listed in Table 2, the thickness increases from 100 nm to 200 nm as long as the In nominal concentration which suggested that the increasing of $InCl_3$ concentration promotes the formation of material compound.

3.3. Morphological study

Fig. 3. exhibits the surface morphology of CIS-1, CIS-3 and CIS-4 samples obtained by SEM. The surface of CIS-1 sample is composed of circular grains, while the morphology of CIS-3 and CIS-4 samples consists of nanotubes. Fig. 3 shows the In nominal concentration has a strong influence on the surface morphology of CIS films grown by CBD. According to structural analysis, previously discussed, the increasing of the In nominal concentration promotes the formation of $CuInS_2$ compound, suggesting that nanotubes observed by SEM in the CIS-4 sample are of $CuInS_2$, while those on the surface of the CIS-3 sample correspond to a mixture of $CuInS_2$ and CuS. Santos et al. [9] report that their CuS thin films have circular grains on the surface, whereas other groups have reported $CuInS_2$ nanotubes on the surface of films [5,6]. Based on this reports we infer that the circular grains of CIS-1 sample are formed mostly of CuS crystals, while nanotubes of the CIS-4 sample of $CuInS_2$ crystals.

3.4. Composition analysis

To quantify the composition of CIS films, EDS measurements were performed using an acceleration voltage of 20 kV. The EDS is a technique that allows a quantitative analysis of the composition of a material. The Cu, In and S atomic concentrations obtained from EDS measurements for CIS-1 and CIS-2 samples are compiled in Table 3. From our Raman study and XRD characterization; CIS-1 and CIS-2 samples have a mixture of $CuInS_2$ and CuS phases, so the Cu atomic concentration measurement by EDS should be divided into two an atom for the formation of $CuInS_2$ compound and one for the formation of CuS. While the sulfur atomic concentration measurements by EDS should be divided into three; two atoms for the formation of the ternary compound and one for the formation of the binary compound. In Table 3 the Cu′=Cu/2 and S′= S/3 ratios as well as S′:Cu′ and 2S′:Cu′ ratios for CIS-1 and CIS-2 samples are compiled. The S′:Cu′ and 2S′:Cu′ ratios of the CIS-1 sample have a value of 1.19 and 2.38 (see Table 3), respectively. The S′:Cu′ and 2S′:Cu′ ratios for the CIS-2 sample was 1.06 and 2.13, respectively (see Table 3). If the S′:Cu′ ratio of CIS-1 and CIS-2 samples has a value of ≈ 1 this would indicate the formation of CuS phase, whereas a value of ≈ 2 in the 2S′:Cu ratio indicates the formation of $CuInS_2$ compound. The Cu, In and S atomic concentration measurements by EDS for the CIS-3 and CIS-4 samples are shown in Table 4. The S:Cu, In:Cu and S:In ratios of the CIS-3 sample were 1.86, 1.06 and 1.73, respectively, while those of the CIS-4 sample were 1.97, 1.09 and 1.80, respectively. From Table 4 note that the S:Cu ratio for the CIS-4 sample has a value close to 2

Table 2
Structural parameters of $CuInS_2$ thin films grown by CBD.

Sample	[$InCl_3$] (M)	Thickness (nm)	Crystalline size (nm)	Dislocation density ($\times 10^{15}$ lines/m^2)	Microstrain ($\times 10^{-3}$)
CIS-1	0.002	100	22.49	1.98	5.07
CIS-2	0.010	158	16.54	3.65	6.94
CIS-3	0.020	190	14.63	4.67	7.87
CIS-4	0.025	200	13.39	5.58	8.65

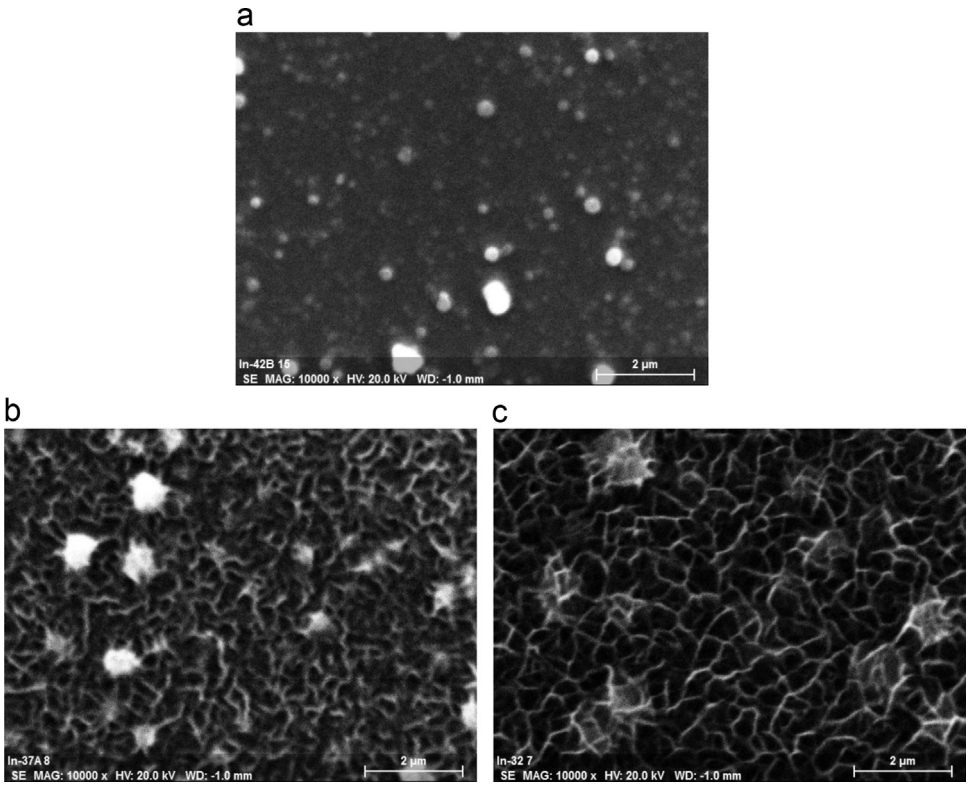

Fig. 3. SEM image of representative CIS samples.

Table 3
Cu, In and S atomic concentrations and stoichiometric analysis for CIS-1 and CIS-2 samples.

Sample	Cu (%)	In (%)	S (%)	Cu′ (%)	S′ (%)	S′:In	S′:Cu′	2S′:Cu′
CIS-1	30.33	15.38	54.29	15.16	18.10	1.17	1.19	2.38
CIS-2	29.56	23.21	47.22	14.78	15.74	0.68	1.06	2.13

Table 4
Cu, In and S atomic concentrations, and stoichiometric analysis for CIS-3 and CIS-4 samples.

Sample	Cu (%)	In (%)	S (%)	S:Cu	In:Cu	S:In
CIS-3	25.49	27.20	47.31	1.86	1.06	1.73
CIS-4	24.58	26.91	48.51	1.97	1.09	1.80

(1.97), this shows that the stoichiometry of the CIS-4 sample corresponds to the $CuInS_2$ compound. These results indicate that for low indium nominal concentrations CIS films have a mixture of CuS and $CuInS_2$ phases, while the phase corresponding to binary compound (CuS) disappears after increasing the In nominal concentration. In fact for a 0.025 M $InCl_3$ concentration $CuInS_2$ films were obtained, in agreement with the Raman study and XRD characterization.

3.5. PL characterization

PL spectra at room temperature of CIS films grown by CBD are shown in the Fig. 4. CIS films only have a PL peak at 1.40 eV, which is close to the bandgap energy and can be assigned to a band to band transition [11]. In Fig. 4 the intensity of the PL peak for CIS-1 and CIS-2 samples is very similar. Also observe that the relative intensity of the PL peak increases as the indium nominal concentration increases. The full width at half maximum of the PL

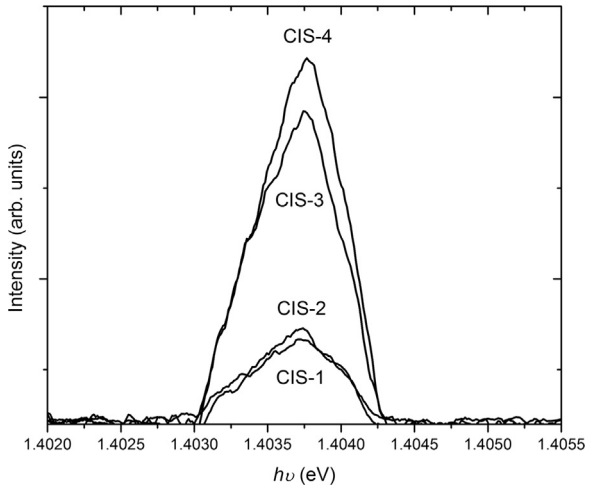

Fig. 4. Photoluminescence spectra at room temperature of CIS films grown by CBD.

peaks (FWHM-PL) decreases as the In nominal concentration increases; the FWHM-PL for CIS-1 and CIS-2 samples were 1.06 eV and 1.05 eV, respectively, while the FWHM-PL for CIS-3 and CIS-4 samples has a value of 0.89 eV and 0.82 eV. The structural and compositional characterization suggested a mixture of CuS and $CuInS_2$ phases in the films, as the $InCl_3$ concentration increases in the bath the formation of $CuInS_2$ compound is promoted until the $CuInS_2$ compound formation. We remark that the reduction of the FWHM-PL is due to an improvement in the crystalline quality of $CuInS_2$ films. Therefore, these results indicate that the quality of the $CuInS_2$ compound improves as the In nominal concentration increases, in agreement with the Raman and XRD analysis. It is important to mention that normally at room temperature $CuInS_2$ films present two distinct emission peaks: a shallow level close to the bandgap and a broad deep level close to 1.13 eV. Our $CuInS_2$

films grown by CBD only have a PL peak close to the bandgap.

4. Conclusions

Copper Indium disulfide thin films grown by CBD were obtained using $CuSO_4$, $InCl_3$ and C_2H_5NS as copper, indium and sulfur sources, respectively. The physical properties were analyzed as a function of the indium nominal concentration. The structural and compositional analyses showed that for low In nominal concentrations the films have a mixture of CuS and $CuInS_2$ phases, while the phase corresponding to binary compound (CuS) disappears after increasing the indium nominal concentration. In fact for a 0.025 M $InCl_3$ concentration $CuInS_2$ films were obtained. The FWHM-PL spectra showed that as the indium nominal concentration increases the crystalline quality of $CuInS_2$ films improves.

Acknowledgments

We acknowledge the technical support of Marcela Guerrero, Paulina González Arceo, A. García-Sotelo and Zacarías Rivera from Physics Department of the CINVESTAV-IPN.

The authors acknowledge financial support for this work from Fondo Sectorial CONACYT-SENER-Sustentabilidad Energética through CeMIE-sol, within the strategic project number 37; "Development of new photovoltaic devices and semi-superconductor materials".

References

[1] Y. Peña, S. Lugo, M. Calixto-Rodríguez, A. Vázquez, I. Gómez, P. Elizondo, App. Surf. Sci. 257 (2011) 2193–2196.
[2] Stefan Seeger, Klaus Ellmer, Thin Solid Films 517 (2009) 3143–3147.
[3] Wen-Jen Tsai, Chia-Hung Tsai, Chih-Hui Chang, Jyh-Ming Ting, Rui-Ren Wang, Thin Solid Films 519 (2010) 1712–1716.
[4] Tomoaki Terasako, Yuji Uno, Seiki Inoue, Tetsuya Kariya, Sho Shirakata, Phys. Stat. Solidi C 3 (8) (2006) 2588–2591.
[5] Ramphal Sharma, Suyeon Shim, Rajaram S. Mane, T. Ganesh, Anil Ghule, Gangri Cai, Duk-Ho Ham, Sun-Ki Min, Wonjoo Lee, Sung-Hwan Han, Mater. Chem. Phys. 116 (2009) 28–33.
[6] Guan-Ting Pan, M.-H. Lai, Rei-Cheng Juang, T.-W. Chung, Thomas C.-K. Yang, Sol. Energy Mater. Sol. Cells 94 (2010) 1790–1796.
[7] K. Kondo, S. Nakamura, K. Sato, Jpn. J. Appl. Phys. 37 (1998) 5728–5729.
[8] Michel H.C. Jin, Kulbinder K. Banger, Jerry D. Harris, Aloysius F. Hepp, Mater. Sci. Eng. – B 116 (2005) 39–401.
[9] J. Santos-Cruz, S.A. Mayén-Hernández, J.J. Coronel-Hernández, R. Mejía-Rodríguez, R. Castanedo-Pérez, G. Torres-Delgado, S. Jiménez-Sandoval, Chalcogenide Lett. 9 (2012) 85–91.
[10] A. Neisser, I. Hengel, R. Klenk, Th.W. Matthes, J. Álvarez-García, A. Pérez-Rodríguez, A. Romano-Rodríguez, M.-Ch Lux-Steiner, Sol. Energy Mater. Sol. Cells 67 (2001) 97–104.
[11] Stefan Seeger, Klaus Ellmer, Thin Solid Films 517 (2009) 3143–3147.